EURASIP Journal on Wireless Communications and Networking

RESEARCH Open Access

Intelligent power optimization for capacity maximization in IRS-assisted NOMA networks

Mohammed H. Alsharif[1*], Abu Jahid[2], Hala Mostafa[3], Mohamed Marey[4] and Mun-Kyeom Kim[5*]

*Correspondence:
malsharif@sejong.ac.kr;
mkim@cau.ac.kr

[1] Department of AI Convergence Electronic Engineering, Sejong University, Seoul 05006, Korea
[2] School of Electrical Engineering and Computer Science, University of Ottawa, 25 Templeton St., Ottawa, ON K1N 6N5, Canada
[3] Department of Information Technology, College of Computer and Information Sciences, Princess Nourah bint Abdulrahman University, P.O. Box 84428, Riyadh 11671, Saudi Arabia
[4] Department of Electronics and Electrical Engineering, Misr University, 6 Octobar, Egypt
[5] School of Energy System Engineering, Chung-Ang University, 84 Heukseok-Ro, Dongjak-Gu, Seoul 06974, Republic of Korea

Abstract

This paper explores the performance of non-orthogonal multiple access (NOMA) in networks enhanced by intelligent reflecting surfaces, with a particular focus on optimizing power allocation to balance system capacity and user fairness. This article derives the optimal power allocation strategy and employs Karush–Kuhn–Tucker conditions to analytically solve the optimization problem. MATLAB simulations are used to validate the approach, ensuring both users meet their minimum data rate requirements under total power constraints. Results show that the optimal power allocation strategy prioritizes the weaker user (UE2) to ensure fairness while maintaining a sufficient capacity margin for the stronger user (UE1). As total power increases, the achievable capacity of UE1 grows logarithmically, reaching 19.41 bps/Hz at 20W, while UE2's capacity initially increases but saturates around 1.74 bps/Hz due to interference from UE1. Consequently, total system capacity exhibits diminishing returns, increasing from 19.122 bps/Hz at 5W to 21.132 bps/Hz at 20W. Further analysis reveals that as UE1's power increases, interference to UE2 rises, limiting its capacity growth. Despite this, optimization ensures both users meet their minimum capacity requirements, demonstrating the efficiency of NOMA in managing power distribution and interference.

Keywords: NOMA, IRS-assisted networks, Power allocation optimization, Spectral efficiency, User fairness, Capacity optimization, Wireless resource allocation

1 Introduction

1.1 Background and motivation

The rapid evolution of wireless communication systems has led to an increasing demand for high spectral efficiency, improved user fairness, and optimized resource allocation. Traditional orthogonal multiple access (OMA) techniques struggle to meet these requirements due to their inherent limitations in spectrum utilization [1]. As a result, Non-Orthogonal Multiple Access (NOMA) has emerged as a promising solution, enabling multiple users to share the same frequency and time resources by leveraging power domain multiplexing [2]. This allows for significant improvements in spectral efficiency and accommodates a greater number of users compared to conventional OMA schemes. In parallel, Intelligent Reflecting Surfaces (IRS) have gained attention as a transformative technology capable of enhancing wireless signal propagation through passive

beamforming [3, 4]. By intelligently adjusting the phase shifts of reflected signals, IRS can improve channel conditions, mitigate interference, and enhance system performance. Integrating IRS with NOMA presents an opportunity to further optimize power allocation, improve user fairness, and maximize overall system capacity [5, 6]. However, managing interference, ensuring optimal power distribution, and maintaining quality of service (QoS) requirements for all users remain key challenges in IRS-assisted NOMA systems.

This study is motivated by the need to address these challenges through a comprehensive analysis of power allocation strategies in IRS-assisted NOMA networks. Specifically, we investigate how optimal power allocation affects system capacity, the trade-offs between throughput and fairness, and the impact of interference management on overall network performance. By evaluating the achievable capacities of strong and weak users under different power levels, we aim to develop an effective resource allocation framework that balances efficiency and fairness in next-generation wireless networks.

1.2 Related works and our contributions

NOMA has emerged as a key enabler for improving spectral efficiency and user fairness in next-generation wireless systems. Extensive research has been conducted to optimize power allocation strategies in NOMA systems, both with and without the assistance of IRS.

Initial studies [7–12] explored optimal power allocation to maximize the sum rate in NOMA under the assumption of perfect Successive Interference Cancellation (SIC). These works focus on fairness or capacity but do not consider the practical challenges of residual interference. Subsequent studies [13–23] addressed issues such as imperfect SIC, secure transmission, and energy efficiency. For example, [13] proposed iterative power allocation under imperfect SIC, while [14–16] introduced multi-objective formulations accounting for QoS and fairness constraints. However, most of these studies assume traditional NOMA environments without the added complexity of IRS. More recently, IRS-assisted NOMA has gained traction due to its potential to reconfigure wireless propagation environments and enhance system capacity. Studies such as [24–26] investigated beamforming and deployment strategies for IRS in NOMA networks. However, these works primarily focus on heuristic beamforming or energy-efficient design, often overlooking optimal power allocation and the impact of practical constraints such as QoS guarantees and residual interference.

Unlike prior literature, this work integrates IRS beamforming effects into the analytical optimization of power allocation using the Karush–Kuhn–Tucker (KKT) framework. Our formulation explicitly accounts for both direct and IRS-reflected channels, and considers fairness, interference, and power budget constraints. To the best of our knowledge, no previous work has derived and solved an analytical optimization problem for power allocation in IRS-assisted NOMA networks under these conditions. Table 1 presents a comparison of related studies on power allocation in the NOMA system.

While prior works such as [22–24] have focused on IRS beamforming in NOMA networks, they often rely on heuristic or simulation-based methods without offering rigorous analytical formulations for power allocation. In contrast, our work formulates the power allocation problem under QoS and interference constraints and solves it

Table 1 Comparison of related studies on power allocation in NOMA system

References	Main focus	Key contribution
[7–11]	Power allocation in NOMA with perfect SIC	Optimized sum capacity and fairness under ideal SIC conditions
[12]	Two-user NOMA with imperfect SIC	Iterative optimization with minimum QoS constraints
[13]	Power allocation with QoS in multi-user NOMA	Alternating maximization with CSI-based power control
[14]	Secure transmission in NOMA with imperfect CSI	Secrecy rate maximization under power and QoS constraints
[15]	Multi-objective optimization for rate and power	Trade-off analysis for sum rate and transmit power
[16]	Power and frequency allocation in downlink NOMA	Resource allocation considering SIC and user rate needs
[17]	Weighted sum rate in multi-carrier NOMA with imperfect SIC	Low-complexity algorithm for power control
[18]	Sum rate maximization in cooperative IRS-aided NOMA	Beamforming and power control using STAR-RIS
[19]	Fairness optimization in NOMA	Power allocation for fairness enhancement
[20]	Proportional fairness in NOMA networks	Tree-search-based user pairing and allocation
[21]	Wireless-powered NOMA fairness	Enhanced fairness under energy harvesting scenarios
[22–24]	IRS beamforming in NOMA systems	Enhancing signal propagation using IRS-based reflection control
This work	Optimal power allocation in IRS-assisted NOMA networks	Analytical KKT-based solution with fairness, interference, and QoS constraints

analytically using the KKT conditions. The main contributions of this research are as follows:

- Derive and analyze the optimal power allocation strategy for NOMA users in an IRS-assisted environment, ensuring that both strong and weak users meet their minimum capacity requirements while maximizing overall system efficiency.
- Derive the Karush–Kuhn–Tucker (KKT) conditions to analytically solve the optimization problem, offering deeper insights into the relationship between power allocation, interference management, and user fairness.
- Utilize MATLAB simulations to solve the optimization problem aimed at maximizing system capacity, while ensuring optimal power allocation for NOMA users in an IRS-assisted environment, subject to total power constraints and minimum data rate requirements to guarantee fairness and quality of service.

By addressing these aspects, this work contributes to a deeper understanding of IRS-assisted NOMA systems and provides a foundation for future research on advanced power control, interference management, and resource allocation strategies in next-generation wireless networks.

1.3 Paper organization

The remainder of this paper is organized as follows: Sect. 2 provides a detailed system model and problem formulation. Section 3 describes the optimization framework, including the derivation of the Karush–Kuhn–Tucker (KKT) conditions. Section 4 presents and

analyzes the simulation results, highlighting the achieved performance improvements. Finally, Sect. 5 concludes the paper.

2 Methods

This section provides a detailed description of the study design, including the system model, channel assumptions, power allocation strategy, and performance metrics. The simulation setup and analysis methods are clearly outlined, ensuring reproducibility and transparency in the evaluation of the IRS-assisted NOMA system. Below is a detailed discussion.

2.1 System model

The system model of the NOMA over IRS-Assisted networks is depicted in Fig. 1. A detailed explanation of the system model is provided in the subsequent paragraphs.

The BS transmits a superimposed signal that is a combination of the signals intended for both users. The transmitted signal can be represented as,

$$x = \sqrt{P_1}s_1 + \sqrt{P_2}s_2 \tag{1}$$

where s_1 and s_2 are the signals for UE1 and UE2, respectively, and P_1 and P_2 are the allocated powers with $P_1 < P_2$. The signal received by UE_1 is,

$$y_1 = h_{1,d}\left(\sqrt{P_1}s_1 + \sqrt{P_2}s_2\right) + G\theta h_{1,r}\left(\sqrt{P_1}s_1 + \sqrt{P_2}s_2\right) + n \tag{2}$$

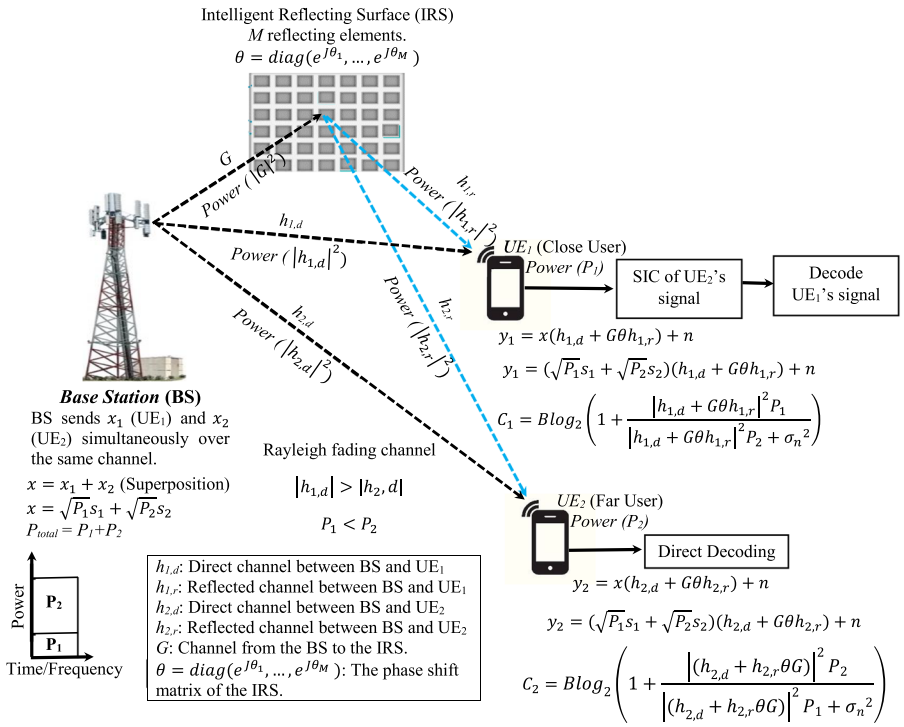

Fig. 1 System model of NOMA over IRS-Assisted networks

$$y_1 = \left(h_{1,d} + G\theta h_{1,r}\right)\left(\sqrt{P_1}s_1 + \sqrt{P_2}s_2\right) + n \tag{3}$$

where $h_{1,\mathrm{d}}$ represents the direct Rayleigh fading channel between BS and UE1, $h_{1,\mathrm{r}}$ represents the reflected channel between IRS and UE1, G represents the channel between BS and IRS, θ represents the phase shift matrix of the IRS, and n is additive white Gaussian noise (AWGN) with mean zero ($\mu = 0$) and variance ${\sigma_n}^2$, $n \sim N(0, {\sigma_n}^2)$. Successive Interference Cancellation (SIC) is employed at UE1's receiver to decode its signal. Specifically, UE1 initially decodes UE2's signal, treating its own signal as interference. This step leverages the fact that UE2's signal is allocated higher power, making it easier to decode. The signal-to-interference-plus-noise ratio (SINR) for decoding s_2 at UE 1 is,

$$\mathrm{SINR}_{2,1} = \frac{\left|(h_{1,d} + h_{1,r}\theta G)\right|^2 P_2}{\left|(h_{1,d} + h_{1,r}\theta G)\right|^2 P_1 + {\sigma_n}^2} \tag{4}$$

Once UE1 successfully decodes s_2, it subtracts (cancels) the decoded s_2 from the received signal y_1. The remaining signal is,

$$y_1\prime = y_1 - \left(h_{1,d} + G\theta h_{1,r}\right)\sqrt{P_2}\widehat{s_2} = \left(h_{1,d} + G\theta h_{1,r}\right)\sqrt{P_1}s_1 + n \tag{5}$$

where $\widehat{s_2}$ is the decoded signal for UE2. After canceling UE2's signal, UE1 can now decode its own signal s_1 from the remaining signal $y_1\prime$. The SINR for decoding s_1 is,

$$\mathrm{SINR}_{1,1} = \frac{\left|(h_{1,d} + h_{1,r}\theta G)\right|^2 P_1}{{\sigma_n}^2} \tag{6}$$

Therefore, the achievable rate for UE1 (C_1) is given by:

$$C_1 = B\log_2\left(1 + \frac{\left|(h_{1,d} + h_{1,r}\theta G)\right|^2 P_1}{{\sigma_n}^2}\right) \tag{7}$$

For UE2, the received signal is expressed as,

$$y_2 = \left(h_{2,d} + G\theta h_{2,r}\right)\left(\sqrt{P_1}s_1 + \sqrt{P_2}s_2\right) + n \tag{8}$$

where $h_{2,\mathrm{d}}$ represents the direct Rayleigh fading channel between BS and UE2, and $h_{2,\mathrm{r}}$ represents the reflected channel between IRS and UE2. As the weak user in a NOMA system, UE2 directly decodes its signal, benefiting from a higher power allocation compared to UE1. This enhanced power allocation enables UE2 to decode its signal first. However, UE2 is unable to separate the signals without performing interference cancellation. The capacity of UE2 is derived using the Shannon capacity formula for a communication channel subject to interference, which is given by:

$$C_2 = B\log_2\left(1 + \frac{\left|(h_{2,d} + h_{2,r}\theta G)\right|^2 P_2}{\left|(h_{2,d} + h_{2,r}\theta G)\right|^2 P_1 + {\sigma_n}^2}\right) \tag{9}$$

The capacity depends on multiple factors, including their channel gains, allocated power, and the noise level in the system. However, power allocation plays a crucial role

in determining the overall system capacity. A user with a stronger channel gain requires less power to achieve reliable communication, while the weaker user benefits from a higher power allocation to mitigate interference from the stronger user. The total capacity is the sum of the individual capacities of both users, as shown below:

$$C_{\text{total}} = B\log_2\left(1 + \frac{\left|(h_{1,d} + h_{1,r}\theta G)\right|^2 P_1}{{\sigma_n}^2}\right) + B\log_2\left(1 + \frac{\left|(h_{2,d} + h_{2,r}\theta G)\right|^2 P_2}{\left|(h_{2,d} + h_{2,r}\theta G)\right|^2 P_1 + {\sigma_n}^2}\right) \tag{10}$$

The total capacity is determined by how power is allocated between users and their individual channel conditions. Proper optimization of power allocation is vital to maximize the overall system capacity. Without efficient power distribution, the system may experience poor performance, either due to insufficient power for the weaker user or excessive interference to the stronger user. In the following section, we will examine the optimization formula for power allocation, aiming to identify the optimal power distribution that maximizes total capacity. This optimization will also consider the balance between improving system performance and ensuring fairness among users.

2.2 Optimization formula

The objective is to maximize system capacity in bps/Hz by optimizing spectral resource use while ensuring total power limits and minimum data rates for fairness and quality. The optimization problem is formulated as follows:

$$(P) : \arg\max_{P_1,P_2}\left(log_2\left(1 + \frac{\left|(h_{1,d} + h_{1,r}\theta G)\right|^2 P_1}{{\sigma_n}^2}\right) + \log_2\left(1 + \frac{\left|(h_{2,d} + h_{2,r}\theta G)\right|^2 P_2}{\left|(h_{2,d} + h_{2,r}\theta G)\right|^2 P_1 + {\sigma_n}^2}\right)\right) \tag{11}$$

Subject to:

$$P_1 + P_2 = P_{\text{total}}, \tag{11.1}$$

$$\log_2\left(1 + \frac{\left|(h_{1,d} + h_{1,r}\theta G)\right|^2 P_1}{{\sigma_n}^2}\right) \geq C_{1,\min,} \tag{11.2}$$

$$\log_2\left(1 + \frac{\left|(h_{2,d} + h_{2,r}\theta G)\right|^2 P_2}{\left|(h_{2,d} + h_{2,r}\theta G)\right|^2 P_1 + {\sigma_n}^2}\right) \geq C_{2,\min,} \tag{11.3}$$

$$P_1 \geq 0; \ldots\ldots P_2 \geq 0. \tag{11.4}$$

The objective function represents total system capacity as the sum of UE1 and UE2 capacities, assuming $B = 1$Hz to simplify power allocation. The constraint $\sum P_i = P_{\text{total}}$ ensures total power does not exceed the available budget, enabling efficient management. Non-negative power constraints ($P_1 \geq 0$, $P_2 \geq 0$) prevent invalid allocations. Lastly, $C_{1,\min}$ and $C_{2,\min}$ set minimum capacity requirements for fairness and quality of service.

The Karush–Kuhn–Tucker (KKT) conditions provide a systematic framework for solving constrained optimization problems, serving as essential criteria for optimality.

In problems with a nonlinear objective function and both equality and inequality constraints, these conditions help identify the optimal power allocation that maximizes system capacity while satisfying all constraints. The solution process begins by developing the Lagrangian function, which integrates the constraints using Lagrange multipliers to facilitate optimization.

(1) Formula of Lagrangian Function: The Lagrangian function is defined as the objective function plus the sum of each constraint multiplied by its corresponding Lagrange multiplier. This allows the problem to be transformed into an unconstrained optimization problem.

$$\begin{aligned} L = & \log_2\left(1+\frac{\left|(h_{1,d}+h_{1,r}\theta G)\right|^2 P_1}{{\sigma_n}^2}\right)+\log_2\left(1+\frac{\left|(h_{2,d}+h_{2,r}\theta G)\right|^2 P_2}{\left|(h_{2,d}+h_{2,r}\theta G)\right|^2 P_1+{\sigma_n}^2}\right) \\ & -\lambda(P_1+P_2-P_{\text{total}})+\mu_1 P_1+\mu_2 P_2+\mu_3\left(\log_2\left(1+\frac{\left|(h_{1,d}+h_{1,r}\theta G)\right|^2 P_1}{{\sigma_n}^2}\right)-C_{1,\min}\right) \\ & +\mu_4\left(\log_2\left(1+\frac{\left|(h_{2,d}+h_{2,r}\theta G)\right|^2 P_2}{\left|(h_{2,d}+h_{2,r}\theta G)\right|^2 P_1+{\sigma_n}^2}\right)-C_{2,\min}\right) \end{aligned} \tag{12}$$

Here, λ is the Lagrange multiplier for the equality constraint, while μ corresponds to the inequality constraints.

(2) KKT conditions: It are a set of necessary conditions for a solution to be optimal in a constrained optimization problem. These conditions apply to problems where the objective function is nonlinear and there are both equality and inequality constraints. The KKT conditions consist of four key components: primal feasibility, which ensures that all constraints are satisfied; dual feasibility, which requires the Lagrange multipliers to be non-negative; complementary slackness, which ensures that each inequality constraint is either active or its corresponding Lagrange multiplier is zero; and the stationarity condition, which ensures that the gradient of the Lagrangian function with respect to the decision variables is zero at the optimal point. Together, these conditions provide a structured approach to finding the optimal solution, ensuring that all constraints are met while maximizing the objective function.

- Stationarity

Stationarity, in the context of the KKT conditions, refers to the condition that the gradient of the Lagrangian function with respect to the decision variables must be zero at the optimal solution. This means that, at the optimal point, the change in the objective function with respect to any small change in the decision variables (power allocation) must be zero, given that all constraints are satisfied. In other words, stationarity ensures that the current solution is a critical point where the objective function is balanced with the influence of the constraints. This condition is essential for identifying the optimal allocation in optimization problems.

$$\frac{\partial L}{\partial P_1}=0 \tag{13}$$

$$\frac{\frac{|(h_{1,d}+h_{1,r}\theta G)|^2}{{\sigma_n}^2}}{\ln(2)\left(1+\frac{|(h_{1,d}+h_{1,r}\theta G)|^2 P_1}{{\sigma_n}^2}\right)}+\frac{\frac{-P_2|(h_{2,d}+h_{2,r}\theta G)|^4}{\left(|(h_{2,d}+h_{2,r}\theta G)|^2 P_1+{\sigma_n}^2\right)^2}}{\ln(2)\left(1+\frac{|(h_{2,d}+h_{2,r}\theta G)|^2 P_2}{|(h_{2,d}+h_{2,r}\theta G)|^2 P_1+{\sigma_n}^2}\right)}$$
$$-\lambda+\mu_1+\mu_3\left(\frac{\frac{|(h_{1,d}+h_{1,r}\theta G)|^2}{{\sigma_n}^2}}{\ln(2)\left(1+\frac{|(h_{1,d}+h_{1,r}\theta G)|^2 P_1}{{\sigma_n}^2}\right)}\right)+\mu_4\left(\frac{\frac{-P_2|(h_{2,d}+h_{2,r}\theta G)|^4}{\left(|(h_{2,d}+h_{2,r}\theta G)|^2 P_1+{\sigma_n}^2\right)^2}}{\ln(2)\left(1+\frac{|(h_{2,d}+h_{2,r}\theta G)|^2 P_2}{|(h_{2,d}+h_{2,r}\theta G)|^2 P_1+{\sigma_n}^2}\right)}\right)=0 \tag{13.1}$$

$$\frac{|(h_{1,d}+h_{1,r}\theta G)|^2}{\ln(2)\left({\sigma_n}^2+|(h_{1,d}+h_{1,r}\theta G)|^2 P_1\right)}(1+\mu_3)$$
$$+\frac{-P_2|(h_{2,d}+h_{2,r}\theta G)|^4}{\ln(2)\left(|(h_{2,d}+h_{2,r}\theta G)|^2 P_1+{\sigma_n}^2\right)\left(|(h_{2,d}+h_{2,r}\theta G)|^2 P_1+{\sigma_n}^2+P_2|(h_{2,d}+h_{2,r}\theta G)|^2\right)} \tag{13.2}$$
$$(1+\mu_4)=\lambda-\mu_1$$

$$\frac{\partial L}{\partial P_2}=0 \tag{14}$$

$$\frac{\frac{|(h_{2,d}+h_{2,r}\theta G)|^2}{|(h_{2,d}+h_{2,r}\theta G)|^2 P_1+{\sigma_n}^2}}{\ln(2)\left(1+\frac{|(h_{2,d}+h_{2,r}\theta G)|^2 P_2}{|(h_{2,d}+h_{2,r}\theta G)|^2 P_1+{\sigma_n}^2}\right)}-\lambda+\mu_2+\mu_4\left(\frac{\frac{|(h_{2,d}+h_{2,r}\theta G)|^2}{|(h_{2,d}+h_{2,r}\theta G)|^2 P_1+{\sigma_n}^2}}{\ln(2)\left(1+\frac{|(h_{2,d}+h_{2,r}\theta G)|^2 P_2}{|(h_{2,d}+h_{2,r}\theta G)|^2 P_1+{\sigma_n}^2}\right)}\right)=0 \tag{14.1}$$

$$\frac{|(h_{2,d}+h_{2,r}\theta G)|^2}{\ln(2)\left(|(h_{2,d}+h_{2,r}\theta G)|^2 P_1+{\sigma_n}^2+|(h_{2,d}+h_{2,r}\theta G)|^2 P_2\right)}(1+\mu_4)=\lambda-\mu_2 \tag{14.2}$$

$$\frac{\partial L}{\partial \lambda}=0 \tag{15}$$

$$P_1+P_2=P_{\text{total}} \tag{15.1}$$

- Complementary slackness conditions

The complementary slackness conditions are a crucial part of the KKT conditions. They ensure that for each inequality constraint in the optimization problem, either the constraint is active (i.e., satisfied with equality) or its corresponding Lagrange multiplier is zero. In other words, if a constraint is not active (i.e., the inequality is strictly satisfied), the Lagrange multiplier associated with that constraint must be zero. Conversely, if the constraint is active (i.e., the inequality holds as equality), the Lagrange multiplier can be positive. These conditions help identify the critical points in the optimization process, where the constraints directly influence the solution, guiding the allocation of resources in optimal power distribution and similar problems.

$$\mu_1 P_1=0, \tag{16}$$

$$\mu_2 P_2=0, \tag{17}$$

$$\mu_3\left(\log_2\left(1+\frac{\left|(h_{1,d}+h_{1,r}\theta G)\right|^2 P_1}{{\sigma_n}^2}\right)-C_{1,\min}\right)=0, \tag{18}$$

$$\mu_4\left(\log_2\left(1+\frac{\left|(h_{2,d}+h_{2,r}\theta G)\right|^2 P_2}{\left|(h_{2,d}+h_{2,r}\theta G)\right|^2 P_1+{\sigma_n}^2}\right)-C_{2,\min}\right)=0. \tag{19}$$

- Primal feasibility conditions

Primal feasibility conditions are part of the KKT conditions and ensure that the solution to the optimization problem satisfies all the constraints. Specifically, for an optimization problem with inequality and equality constraints, the primal feasibility conditions require that the decision variables lie within the feasible region defined by these constraints. In other words, for all inequality constraints, the decision variables must meet or exceed the lower bounds, and for equality constraints, the decision variables must satisfy the exact equality. These conditions guarantee that the solution respects the limitations set by the problem and is feasible in the original problem space.

$$P_1+P_2=P_{\text{total}} \tag{20}$$

$$P_1\geq 0, P_2\geq 0 \tag{21}$$

$$\log_2\left(1+\frac{\left|(h_{1,d}+h_{1,r}\theta G)\right|^2 P_1}{{\sigma_n}^2}\right)\geq C_{1,\min,} \tag{22}$$

$$\log_2\left(1+\frac{\left|(h_{2,d}+h_{2,r}\theta G)\right|^2 P_2}{\left|(h_{2,d}+h_{2,r}\theta G)\right|^2 P_1+{\sigma_n}^2}\right)\geq C_{2,\min,} \tag{23}$$

- Dual feasibility conditions

Dual feasibility conditions are a key component of the KKT conditions. They ensure that the Lagrange multipliers associated with the inequality constraints are non-negative. Specifically, for each inequality constraint in the optimization problem, the corresponding Lagrange multiplier must be greater than or equal to zero. This condition

Table 2 Simulation setup

Parameter	Value
Fading channel realization (N)	1000
Minimum data rate for UE1 ($C1_{,\min}$)	1 bps/Hz
Minimum data rate for UE2 ($C2_{,\min}$)	0.5 bps/Hz
Total power budget of BS (P_{total})	1 to 20 Watt (30 to 43 dB_m)
Noise	0.0001 Watt
Number of IRS elements (M)	10
Θ	$\theta=\text{diag}(e^{J\theta_1},\ldots,e^{J\theta_M})$

Table 3 Table of symbols

Symbol	Description
x_1	Transmit data to UE_1
P_1	Transmit power of UE_1
$h_{1,d}$	Fading channel between BS and UE_1
C_1	Capacity of UE_1
x_2	Transmit data to UE_2
P_2	Transmit power of UE_2
$h_{2,d}$	Fading channel between BS and UE_2
C_2	Capacity of UE_2
C_{min}	Minimum capacity required
$h_{1,r}$	Reflected channel between BS and UE_1
$h_{2,r}$	Reflected channel between BS and UE_2
G	Channel from the BS to the IRS
Θ	$\theta = diag(e^{J\theta_1}, \ldots, e^{J\theta_M})$: The phase shift matrix of the IRS
P_{total}	Total transmit power of BS
C_{total}	Total system capacity
B	Bandwidth
n	Additive white Gaussian noise (AWGN)
$N(0, {\sigma_n}^2)$	Normal Gaussian distribution with zero mean and variance ${\sigma_n}^2$
Λ	Lagrange multiplier for the equality constraint
μ	Lagrange multiplier for the inequality constraints

reflects that the Lagrange multipliers represent the sensitivity of the objective function to the constraints, and their non-negativity indicates that the constraints are either binding (active) or not affecting the solution. Dual feasibility guarantees that the optimization respects the constraints and that the solution is valid in the dual space of the problem.

$$\mu_1 \geq 0, \mu_2 \geq 0, \mu_3 \geq 0, \mu_4 \geq 0.$$

The KKT conditions define the equations and inequalities that the optimal solution (P_1, P_2) and Lagrange multipliers ($\lambda, \mu_1, \mu_2, \mu_3, \mu_4$) must satisfy. The solution process involves: (1) solving the stationarity conditions for P_1 and P_2, (2) applying complementary slackness to identify active constraints, and (3) solving the resulting system either numerically or analytically. Due to the nonlinearity and computational complexity of the optimization problem, the solution is obtained through simulation using MATLAB, with the simulation parameters provided in Table 2 and a summary of key symbols presented in Table 3.

3 Results and discussion

This section discusses the performance of NOMA over IRS-Assisted Networks, with a focus on optimal power allocation, capacity optimization, and the trade-offs between system throughput and user fairness. As illustrated in Fig. 2, the power distribution between two users, UE1 and UE2, is analyzed as the total power P_{total} increases from 1 to 20 watts. A key observation is that UE2, which has a weaker channel gain, consistently receives a larger share of the power compared to UE1. This aligns with the fundamental principle of NOMA, where users with poorer channel conditions are prioritized to enhance fairness and maximize overall system efficiency. Allocating more power to UE2

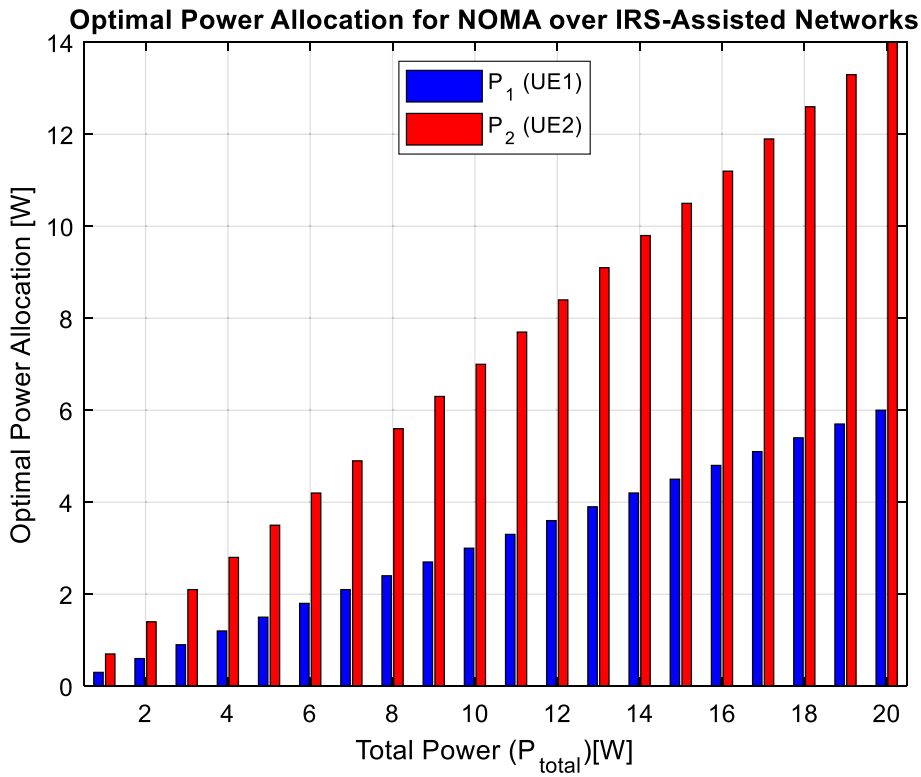

Fig. 2 Optimal power allocation for NOMA over IRS-Assisted networks

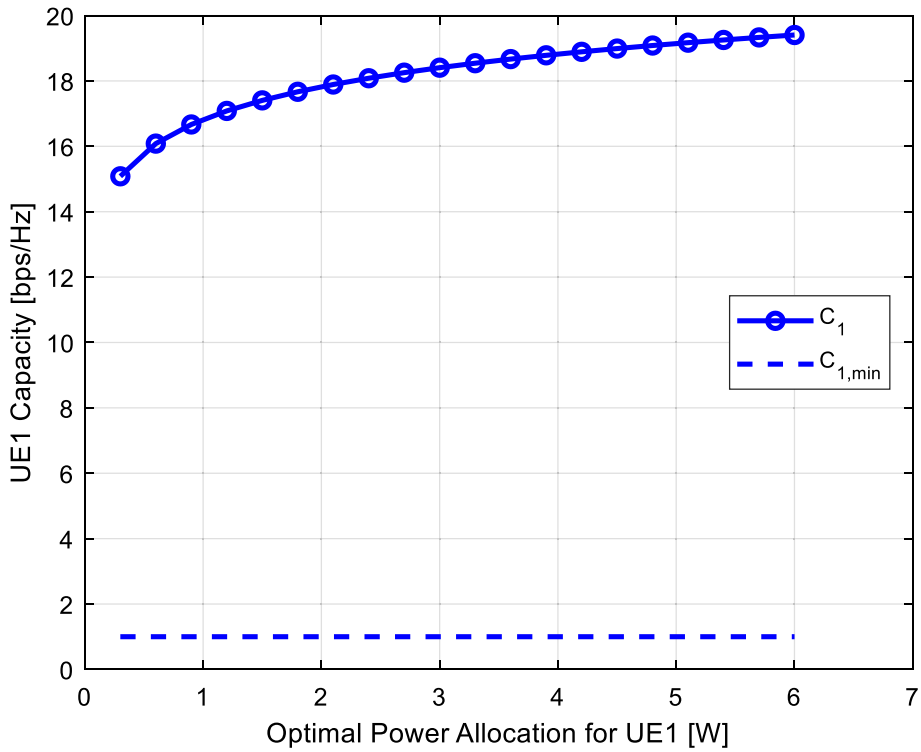

Fig. 3 Optimal power allocation and capacity for UE1

ensures that it meets its minimum capacity requirement $C_{2,\min}$ despite its weaker channel quality.

On the other hand, UE1, which benefits from a stronger channel gain, can achieve its minimum capacity requirement $C_{1,\min}$ with less power. This is due to its ability to handle interference from the weaker user (UE2) using SIC and leverage advanced modulation schemes. Additionally, the nonlinear power allocation pattern highlights the impact of optimization constraints and the interaction of interference between users, which play a crucial role in NOMA over IRS-Assisted Networks. These findings underscore the importance of effective power control strategies in achieving a balance between user fairness and overall system performance.

Figure 3 illustrates the relationship between the optimal power allocation for UE1 (P_1^{opt}) and its corresponding capacity (C_1), alongside the minimum capacity requirement ($C_{1,\min}=1$ bps/Hz), which is set to maintain a high Quality of Service (QoS) for UE1. As P_1^{opt} increases, C_1 exhibits a logarithmic growth, highlighting the direct influence of power allocation on UE1's capacity. Notably, C_1 consistently remains above or equal to $C_{1,\min}$, ensuring that UE1's QoS requirements are continuously met. This is achieved through an optimized power allocation strategy that balances the needs of both UE1 and UE2, ensuring sufficient power is allocated to UE1 while maintaining overall system efficiency.

The figure also demonstrates that for $P_{\text{total}}=5$ watts, $P_1^{\text{opt}}=1.504$ watts, resulting in $C_1=17.401$ bps/Hz, which significantly exceeds the minimum capacity requirement. Similarly, when P_{total} increases to 10 watts, P_1^{opt} rises to 3.042 watts, with $C_1=18.410$ bps/Hz, further demonstrating the system's ability to maintain high QoS for UE1. As

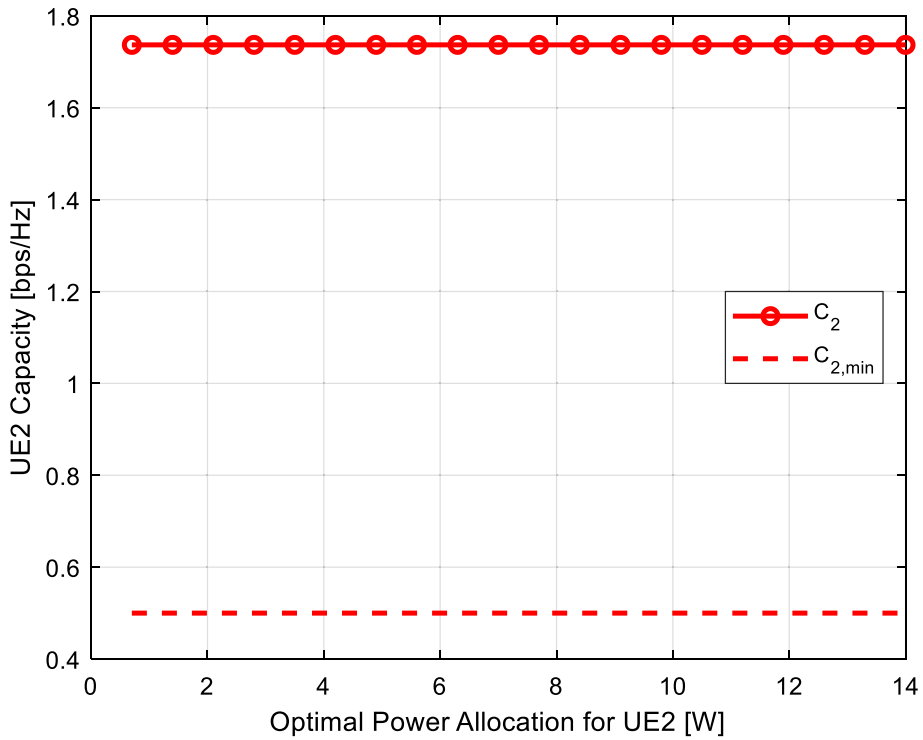

Fig. 4 Optimal power allocation and capacity for UE2

P_{total} continues to increase, reaching 15 and 20 watts, P_1^{opt} increases to 4.505 and 6.001 watts, respectively, leading to a corresponding rise in C_1 to 18.99 and 19.41 bps/Hz. This steady increase in capacity is primarily attributed to the effectiveness of SIC in mitigating interference from UE2, allowing UE1 to maintain high spectral efficiency. These results emphasize the crucial role of power optimization and SIC in ensuring reliable and efficient performance in NOMA over IRS-Assisted Networks.

Figure 4 shows the relationship between the optimal power allocation for UE2 (P_2^{opt}) and its capacity (C_2), alongside the minimum capacity requirement ($C_{2,\text{min}}=0.5$ bps/Hz). As P_2^{opt} increases, C_2 also grows, demonstrating the impact of power allocation on UE2's capacity. However, C_2 increases at a slower rate than UE1 due to interference from UE1, a characteristic of NOMA systems. The dashed red line represents $C_{2,\text{min}}$, ensuring UE2 can support basic services like web browsing or messaging. The system maintains C_2 above $C_{2,\text{min}}$ by carefully distributing power between UE1 and UE2.

For instance, at $P_{\text{total}}=5$ watts, $P_2^{\text{opt}}=3.490$ watts results in $C_2=1.736$ bps/Hz, exceeding the minimum requirement. Similarly, with $P_{\text{total}}=10$ watts, $P_2^{\text{opt}}=6.979$ watts provides $C_2=1.74$ bps/Hz, consistently meeting UE2's QoS needs. When P_{total} increases to 15 and 20 watts, P_2^{opt} rises to 10.49 and 13.99 watts, respectively, but C_2 remains nearly constant around 1.74 bps/Hz. This plateau occurs because the increased power for UE1 enhances interference for UE2, neutralizing the gains from additional power allocated to UE2 and resulting in a stable capacity at higher power levels.

Figure 5 presents the achievable capacities and the total power. As P_{total} increases, C_1 grows logarithmically, reaching 17.401 bps/Hz at 5W, 18.410 bps/Hz at 10W, and

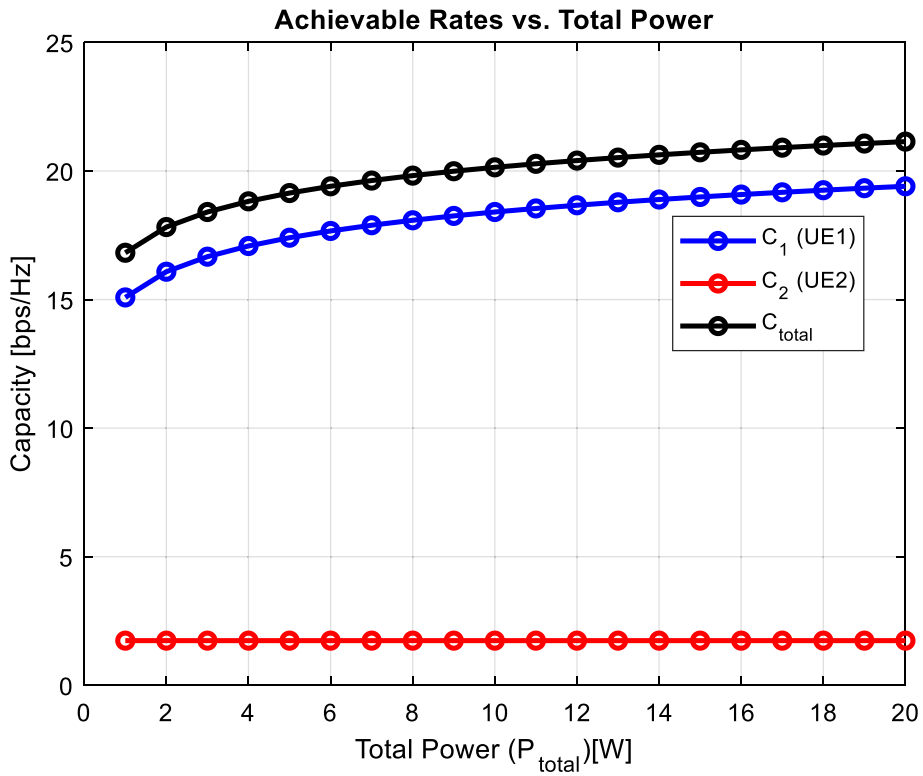

Fig. 5 Achievable capacities versus total power

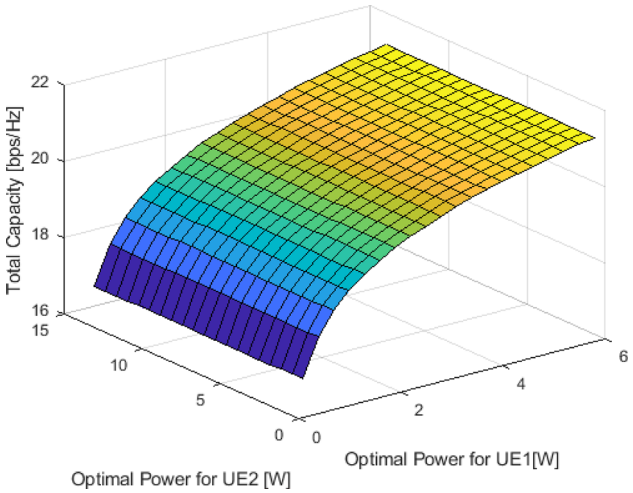

Fig. 6 Optimal power allocation for UE1, UE2, and total system capacity

Table 4 A comparison with three key related works

Criteria	[11]	[12]	[23]	This article
Main Contributions	Power allocation (PA) lookup tables Capacity–BER trade-off SIC considered Simulation-based validation	Joint fairness + sum rate optimization KKT-based iterative PA Fairness metric (Jain's index)	Two-stage Subchannel Allocation (SA) + PA approach Enforces SIC via power gap Evaluated using 4 heuristic SA methods	First closed-form PA via KKT for IRS-NOMA Includes direct + reflected channels Guarantees fairness, QoS, and interference limits
Optimization	Simulation-based search No analytical solution	Weighted-sum scalarization KKT conditions	Heuristic SA + linear PA Convex optimization	Full analytical KKT-based PA Includes fairness, interference, and QoS
Fairness Handling	Indirect via BER constraints	Explicit (Jain's index + weights)	Resource-limited fairness User assignment	Explicit constraints Prioritizes weaker user
Simulation Results	Capacity–BER trade-off Lookup table results	Fairness–rate trade-off curves 5.28 bps/Hz (3 users)	SA/PA comparison across algorithms 11.17 bps/Hz (WSA algorithm)	Best sum capacity: 21.13 bps/Hz at 20W (Fig. 5)

19.41 bps/Hz at 20W, benefiting from SIC. In contrast, C_2 rises initially (1.736 bps/Hz at 5W) but stagnates around 1.74 bps/Hz at higher power levels due to increasing interference from UE1. Consequently, total capacity C_{total} is primarily influenced by C_1, increasing significantly at lower power levels but showing diminishing returns as C_2 saturates. For instance, at $P_{\text{total}} = 5$ watts, $C_{\text{total}} = 19.122$ bps/Hz, which increases to 20.132 bps/Hz at 10 watts, 20.712 bps/Hz at 15 watts, and 21.132 bps/Hz at 20 watts. This trend highlights a key trade-off in NOMA over IRS-assisted networks: while increasing power improves total system capacity, interference limits the capacity growth of the weaker user. Therefore, optimizing power allocation and interference mitigation strategies, such as IRS beamforming and advanced SIC techniques, is essential for maximizing overall system performance.

Figure 6 illustrates the relationship between the optimal power allocation for UE1 (P_1^{opt}), UE2 (P_2^{opt}), and total system capacity (C_{total}), highlighting the impact of power distribution on NOMA performance. As P_1^{opt} and P_2^{opt} increase, C_{total} generally improves, demonstrating the benefits of higher power allocation. However, the trade-off between UE1 and UE2 is carefully optimized to ensure both meet their minimum capacity requirements ($C_{1,\min} = 1$ bps/Hz, $C_{2,\min} = 0.5$ bps/Hz) while maximizing C_{total}. At $P_{\text{total}} = 10$ watts, $P_1^{\text{opt}} = 3.043$ watts, $P_2^{\text{opt}} = 6.979$ watts, and $C_{\text{total}} = 20.14$ bps/Hz. In addition, Fig. 6 also reflects the impact of interference, as increasing P_1^{opt} raises interference for UE2, limiting C_{total} at higher power levels. Despite this, the system ensures both users achieve their QoS requirements, demonstrating NOMA's effectiveness in balancing power allocation and interference management, making it a reliable and efficient solution for modern wireless networks.

Ultimately, Table 4 presents a comparison with three key related works, focusing on core contributions, optimization approaches, fairness mechanisms, and achieved performance metrics.

4 Conclusion and future research

This study provided an in-depth analysis of optimal power allocation in IRS-assisted NOMA networks, focusing on capacity optimization, user fairness, and interference management. Through mathematical modeling and optimization, we derived power allocation strategies ensuring that both the strong user (UE1) and weak user (UE2) meet their minimum capacity requirements while maximizing overall system performance. The results showed that as total power (P_{total}) increases, the capacity of UE1 grows logarithmically, while the capacity of UE2 remains nearly constant at higher power levels due to increased interference from UE1. Numerical results demonstrated the impact of power allocation on system performance. For instance, at $P_{\text{total}} = 10$ watts, the optimal power allocations were $P_1^{\text{opt}} = 3.043$ watts, $P_2^{\text{opt}} = 6.979$ watts, resulting in total system capacity $C_{\text{total}} = 20.14$ bps/Hz. Similarly, at $P_{\text{total}} = 20$ watts P_1^{opt} increased to 6.001 watts and P_2^{opt} to 13.94 watts, yielding $C_{\text{total}} = 21.132$ bps/Hz. However, despite the increased power allocation to UE2, its capacity remained nearly constant around 1.74 bps/Hz due to the growing interference from UE1, highlighting the limitations imposed by inter-user interference.

Future research can extend this study by exploring:

1. Optimized beamforming and power allocation strategies for maximizing spectral efficiency in near-field communication environments of IRS-assisted NOMA networks. As wireless systems evolve toward 6G, the operating frequencies are expected to increase into the millimeter-wave and terahertz bands, where the communication distances often fall within the electromagnetic near-field region. In this regime, the traditional far-field assumptions no longer hold, and the wavefronts become spherical rather than planar. This fundamental shift in channel modeling introduces new design challenges, particularly in terms of beamforming, as spatial focusing becomes critical for directing energy efficiently to users. When IRS is incorporated into this setup, its potential for intelligent signal reflection and spatial reconfiguration becomes even more pronounced in the near-field, offering the ability to finely control the directionality and intensity of the reflected signals.

Combining this with NOMA adds further complexity due to the need for superposition coding and SIC, requiring careful user pairing and interference management. In such scenarios, it becomes essential to jointly optimize the transmit beamforming at the base station, the power allocated to each user, and the phase shift configuration of the IRS. The objective is to maximize the overall spectral efficiency while ensuring reliable signal decoding and maintaining user fairness. However, this joint optimization problem is highly non-convex and computationally demanding, especially as the number of users and IRS elements increases. Learning-based techniques such as deep reinforcement learning could be employed to adaptively solve the problem in dynamic environments with partial channel state information.

2. Another promising direction for future research is the development of an efficient optimization framework for phase shift configuration in Stacked Intelligent Metasurfaces (SIM)-assisted Holographic MIMO (HMIMO) systems. This emerging architecture leverages the concept of densely packed and spatially continuous antenna elements, known as holographic MIMO, in conjunction with multiple stacked layers of programmable metasurfaces to enhance wave manipulation capabilities. By introducing stacked intelligent metasurfaces between the transmitter and receiver, the system can harness an ultra-high spatial resolution for beam steering, wavefront shaping, and signal focusing. Such a configuration offers tremendous potential for precise channel control, particularly in rich-scattering or non-line-of-sight (NLoS) environments.

To fully realize these benefits, a critical research task lies in optimizing the phase shifts applied by each layer of the SIM. The primary objective in this context is to minimize the normalized mean squared error (NMSE) associated with channel estimation or signal recovery, thereby ensuring high-fidelity communication. However, this optimization must be carefully designed to comply with several key constraints. First, there is the unit-modulus constraint, which arises because each metasurface element can only adjust the phase not the amplitude of incident signals. This introduces a non-convex constraint that significantly complicates the optimization process. Second, a pilot power constraint must be respected to prevent excessive training overhead, particularly important in systems with large numbers of antennas and reflection elements. Third, a channel estimation constraint must be imposed to ensure that the phase configuration does not compromise the accuracy or robustness of the estimated channel under practical conditions, such as hardware impairments or rapidly varying environments.

Abbreviations

AWGN	Additive white Gaussian noise
QoS	Quality of service
UE	User equipment
OMA	Orthogonal multiple access
NOMA	Non-orthogonal multiple access
IRS	Intelligent reflecting surfaces
CSI	Channel state information
KKT	Karush–Kuhn–Tucker

Acknowledgements

Chung-Ang University Research Grants in 2025. Princess Nourah bint Abdulrahman University Researchers Supporting Project number (PNURSP2025R137), Princess Nourah bint Abdulrahman University, Riyadh, Saudi Arabia.

Author contributions

Conceptualization, MHA and AJ; methodology, HM and MM; investigation, M-KK; software, MHA; validation, M-KK; writing original draft, MHA and AJ; writing review and editing, HM, MM, and M-KK. All authors have read and agreed to the published version of the manuscript.

Funding
This research was supported by the Chung-Ang University Research Grants in 2025. Princess Nourah bint Abdulrahman University Researchers Supporting Project number (PNURSP2025R137), Princess Nourah bint Abdulrahman University, Riyadh, Saudi Arabia.

Availability of data and materials
The data used to support the findings of this study are available from the corresponding authors upon request.

Declarations

Competing interest
The authors declare no conflict of interest.

Received: 19 February 2025 Accepted: 27 August 2025
Published online: 24 September 2025

References

1. M. Abd-Elnaby, G.G. Sedhom, E.-S.M. El-Rabaie, M. Elwekeil, NOMA for 5G and beyond: literature review and novel trends. Wirel. Netw. **29**, 1629–1653 (2023)
2. P.V. Reddy, S. Reddy, S. Reddy, R.D. Sawale, P. Narendar, C. Duggineni, et al., Analytical review on OMA vs. NOMA and challenges implementing NOMA, in *2021 2nd International Conference on Smart Electronics and Communication (ICOSEC)* (2021), pp. 552–556
3. M. Ahmed, S. Raza, A.A. Soofi, F. Khan, W.U. Khan, S.Z.U. Abideen, et al., Active reconfigurable intelligent surfaces: Expanding the frontiers of wireless communication-a survey. IEEE Commun. Surv. Tutor. (2024)
4. S. Sharma, A.K. Mishra, M.H. Kumar, K. Deka, V. Bhatia, IRS-enhanced cooperative NOMA: a contemporary review. IEEE Access (2024)
5. D. Sarkar, S.S. Yadav, V. Pal, N. Kumar, S.K. Patra, A comprehensive survey on IRS-assisted NOMA-based 6G wireless network: design perspectives, challenges and future directions. IEEE Trans. Netw. Serv. Manag. (2024)
6. F. Naeem, G. Kaddoum, S. Khan, K.S. Khan, N. Adam, IRS-empowered 6G networks: deployment strategies, performance optimization, and future research directions. IEEE Access **10**, 118676–118696 (2022)
7. J.A. Oviedo, H.R. Sadjadpour, A fair power allocation approach to NOMA in multiuser SISO systems. IEEE Trans. Veh. Technol. **66**, 7974–7985 (2017)
8. A. Zakeri, M. Moltafet, N. Mokari, Joint radio resource allocation and SIC ordering in NOMA-based networks using submodularity and matching theory. IEEE Trans. Veh. Technol. **68**, 9761–9773 (2019)
9. A. Zakeri, A. Khalili, M.R. Javan, N. Mokari, E. Jorswieck, Robust energy-efficient resource management, SIC ordering, and beamforming design for MC MISO-NOMA enabled 6G. IEEE Trans. Signal Process. **69**, 2481–2498 (2021)
10. J. Cui, Y. Liu, Z. Ding, P. Fan, A. Nallanathan, Optimal user scheduling and power allocation for millimeter wave NOMA systems. IEEE Trans. Wirel. Commun. **17**, 1502–1517 (2017)
11. M.B. Shahab, S.Y. Shin, User pairing and power allocation for non-orthogonal multiple access: capacity maximization under data reliability constraints. Phys. Commun. **30**, 132–144 (2018)
12. S. Trankatwar, P. Wali, Power allocation scheme for sum rate and fairness trade-off in downlink NOMA networks. Comput. Commun. **221**, 78–89 (2024)
13. I.A. Mahady, E. Bedeer, S. Ikki, H. Yanikomeroglu, Sum-rate maximization of NOMA systems under imperfect successive interference cancellation. IEEE Commun. Lett. **23**, 474–477 (2019)
14. Z. Yang, W. Xu, C. Pan, Y. Pan, M. Chen, On the optimality of power allocation for NOMA downlinks with individual QoS constraints. IEEE Commun. Lett. **21**, 1649–1652 (2017)
15. R. Aldebes, K. Dimyati, E. Hanafi, K.A. Noordin, Z. Ding, Multi-stage algorithm for energy efficiency and data rate trade-off in imperfect CSI downlink NOMA systems. Telecommun. Syst. **88**, 1–17 (2025)
16. W.U. Khan, F. Jameel, T. Ristaniemi, S. Khan, G.A.S. Sidhu, J. Liu, Joint spectral and energy efficiency optimization for downlink NOMA networks. IEEE Trans. Cogn. Commun. Netw. **6**, 645–656 (2019)
17. A. Ali, A. Baig, G.M. Awan, W.U. Khan, Z. Ali, G.A.S. Sidhu, Efficient resource management for sum capacity maximization in 5G NOMA systems. Appl. Syst. Innov. **2**, 27 (2019)
18. X. Wang, R. Chen, Y. Xu, Q. Meng, Low-complexity power allocation in NOMA systems with imperfect SIC for maximizing weighted sum-rate. IEEE Access **7**, 94238–94253 (2019)
19. P. Wang, W. Wu, H. Wang, R. Song, Sum rate maximization for cooperative STAR-RISs aided NOMA system. IEEE Wireless Commun. Lett. (2025). https://doi.org/10.1109/LWC.2025.3532027
20. S. Timotheou, I. Krikidis, Fairness for non-orthogonal multiple access in 5G systems. IEEE Signal Process. Lett. **22**, 1647–1651 (2015)
21. M. Abd-Elnaby, Capacity and fairness maximization-based resource allocation for downlink NOMA networks. Comput. Mater. Contin. (2021). https://doi.org/10.32604/cmc.2021.018351
22. J. Ren, X. Lei, P.D. Diamantoulakis, F. Zhou, X. Tang, O.A. Dobre, NOMA for wireless-powered communication networks with buffered sources. IEEE Trans. Veh. Technol. **70**, 9088–9102 (2021)
23. S. Trankatwar, P. Wali, Subchannel and power optimization for sum rate maximization in downlink multicarrier NOMA networks. Phys. Commun. **58**, 102050 (2023)
24. J. Zhu, Y. Huang, J. Wang, K. Navaie, Z. Ding, Power efficient IRS-assisted NOMA. IEEE Trans. Commun. **69**, 900–913 (2020)
25. M. AlaaEldin, E. Alsusa, K.G. Seddik, M. Al-Jarrah, C. Papadias, Optimization of energy-constrained IRS-NOMA using a complex circle manifold approach. IEEE Internet Things J. (2024). https://doi.org/10.1109/JIOT.2024.3427425

26. A. Ihsan, W. Chen, M. Asif, W.U. Khan, Q. Wu, J. Li, Energy-efficient IRS-aided NOMA beamforming for 6G wireless communications. IEEE Trans. Green Commun. Netw. **6**, 1945–1956 (2022)

Publisher's Note